



PERGAMON

Acta mater. 48 (2000) 385–396



www.elsevier.com/locate/actamat

## INTRINSIC DIFFUSION AND KIRKENDALL EFFECT IN Ni–Pd AND Fe–Pd SOLID SOLUTIONS

M. J. H. VAN DAL, M. C. L. P. PLEUMEEKERS, A. A. KODENTSOV and  
F. J. J. VAN LOO†

Laboratory of Solid State and Materials Chemistry, Eindhoven University of Technology, PO Box 513,  
5600 MB Eindhoven, The Netherlands

(Received 7 June 1999; accepted 8 October 1999)

**Abstract**—Intrinsic diffusion and the Kirkendall effect in the Ni–Pd (at 900–1200°C) and Fe–Pd (at 1100°C) solid solution systems were investigated. The diffusion couple technique including incremental and “multi-foil” couples was employed. A theoretical analysis of the Kirkendall effect, which manifests itself by migration of inert markers inside the interdiffusion zone, was performed for a binary solid solution system. It was demonstrated that depending upon the relative mobilities of the components in different parts of the interaction zone of such binary diffusion couples, the appearance of two or more “Kirkendall” planes as marked by inert particles can be expected. This phenomenon, which indeed was predicted and found in the multiphase Ni/Ti diffusion couple, was not observed in the experiments on the single-phase Ni–Pd and Fe–Pd systems. The diffusion process in these binary systems exhibiting a minimum in the liquidus curve was found to show special features with respect to the concentration dependence of the diffusion coefficients. © 2000 Acta Metallurgica Inc. Published by Elsevier Science Ltd. All rights reserved.

**Keywords:** Bulk diffusion; Kirkendall effect; Ni–Pd alloys; Fe–Pd alloys

### 1. INTRODUCTION

The Kirkendall effect, often accompanying interdiffusion in solids, manifests itself in various phenomena such as migration of macroscopic inclusions inside the interaction zone, the development of diffusional porosity, generation of internal stress and even by deformation of the material on a microscopic scale. These diffusion-induced processes are of concern in a wide variety of structures including composite materials, coatings, welded components, thin-film electronic devices and, therefore, a good understanding of the Kirkendall effect is of great importance.

However, it is necessary to realize that the rationalization and description of the Kirkendall effect are by no means trivial. Despite more than half a century of rather intensive work in this field, a number of fundamental questions still remains to be answered. One of them (and, perhaps, the most puzzling one) is concerned with the migration of inert particles (“fiducial markers”) in concentration gradients developing in the interaction zone. Is the Kirkendall plane as marked by inert particles introduced prior to annealing between the initial end

members of a diffusion couple, unique? In other words, could the inert particles placed at the original interface migrate differently inside the zone of interdiffusion, so that two (or more) actual “Kirkendall planes” can be expected?

For binary two-phase systems, the problem has already been analysed theoretically [1]. The conclusion of this work is that, in general, it is necessary to consider two different Kirkendall frames of reference, one for each adjoining phase. It was also shown that, depending upon the intrinsic diffusion coefficients of the components in both phases, the interfacial composition of the diffusion couple and the composition of the end members of the couple, the phase interface must be able to create and annihilate vacancies. The latter means that the vacancy flux can be, in principle, in one sense in one phase and in the other sense in the other phase. As a result, the appearance of more than one plane marked by inert particles is expected inside the interaction zone.

Recently, we found conclusive experimental evidence supporting this idea. It can be appreciated looking at Fig. 1, which represents a typical reaction zone morphology developed in a multiphase Ni/Ti diffusion couple during annealing at 850°C. In this experiment small particles ( $\approx 0.3 \mu\text{m}$ ) of thorium dioxide ( $\text{ThO}_2$ ) were used as inert markers

† To whom all correspondence should be addressed.

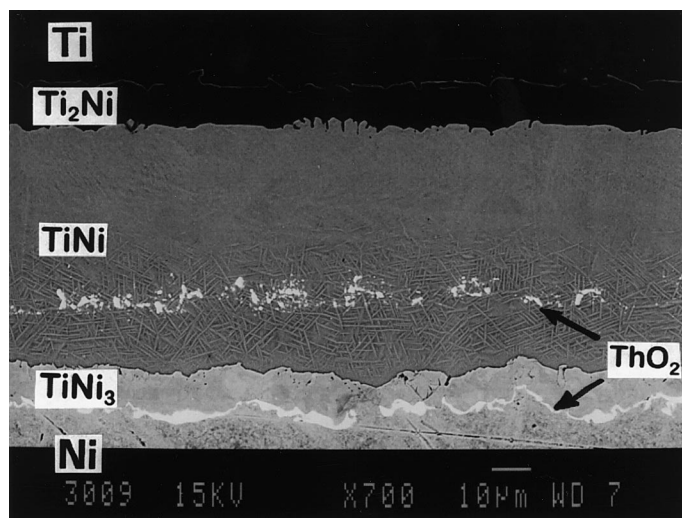


Fig. 1. Backscattered electron image of a cross-section of a Ni/Ti diffusion couple annealed at 850°C for 196 h. ThO<sub>2</sub> particles were used as inert markers between the initial end members. Two “Kirkendall” planes emerged upon the interaction.

between the end members. After interaction the ThO<sub>2</sub> markers can be seen in the TiNi phase as well as at the TiNi<sub>3</sub>/Ni interface, i.e. two “Kirkendall planes” are present.

For the case of a binary system with a continuous solid solution, Cornet and Calais [2] described a hypothetical diffusion couple in which several “Kirkendall planes” can emerge. However, no experimental verification of the model was performed. Therefore, the present work focuses on the interaction in single-phase solid solution systems and seeks to find experimental evidence for the occurrence of a divergence of vacancy fluxes within a disordered phase during the interdiffusion process.

Here, we shall take a closer look at intrinsic diffusion and the Kirkendall effect-related phenomena in two systems, Ni–Pd and Fe–Pd. The diffusion couple technique (including incremental and “multi-foil” couples) was employed in the investigation. These material systems were chosen for several reasons. Firstly, both systems exhibit a minimum in the solidus curve [3] and, therefore, a strong concentration dependence of the mobilities of the species is expected. Secondly, these materials and their alloys are easy to work with, which is essential, especially when “multi-foil” samples are to be made. Furthermore, the availability of thermodynamic data on the binary solid solutions and tracer diffusivities for the entire concentration range of the Fe–Pd alloys (at the temperature of interest) gives an opportunity to test the validity of the Darken equation and reliability of the multi-foil diffusion technique.

The purpose of this paper is threefold:

1. To demonstrate the efficiency of the multi-foil diffusion technique in studying intrinsic diffusion in metallic solid solutions.

2. To perform an experimental and theoretical analysis of interdiffusion in the binary Ni–Pd and Fe–Pd systems over the temperature range 900–1200°C.
3. To contribute to the understanding of the migration of inert markers inside the interdiffusion zone resulting from the Kirkendall effect.

Anticipating the specific results of the present study, it seems worthwhile to give some details about the “multi-foil” diffusion couple technique and to make some general comments concerning the theoretical analysis used.

## 2. THEORETICAL ANALYSIS

### 2.1. The “multi-foil” diffusion couple technique

The “multi-foil” technique for studying interdiffusion phenomena has been introduced by Heumann and Walther [4]. The characteristic feature of a “multi-foil” sample is that each end member of the diffusion couple is composed of several foils with fiducial markers in between. The total number of foils within the end members and their thickness may vary depending on the interaction rate in the material system at the temperature of interest. Interdiffusion in such a multi-layered system will cause the markers to move relative to a laboratory-fixed frame of reference with the so-called Kirkendall velocity  $v$  (m/s). The latter, in the case of a binary A–B multi-foil couple, is dependent on the difference of the intrinsic diffusivities of the species and the concentration gradients developing in the interdiffusion zone [5]:

$$v = V_A(D_A - D_B) \cdot \frac{dC_A}{dx}. \quad (1)$$

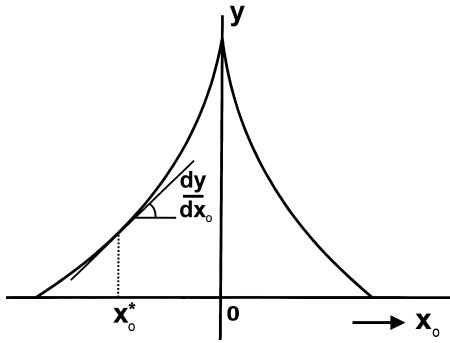


Fig. 2. Schematic representation of marker displacement,  $y$ , vs their original position  $x_0$  in a multi-foil diffusion couple.

Here,  $D_A$  and  $D_B$  are the intrinsic diffusivities ( $\text{m}^2/\text{s}$ ),  $V_A$  is the partial molar volume ( $\text{m}^3/\text{mol}$ ),  $C_A$  is the concentration of component A ( $\text{mol}/\text{m}^3$ ) and  $x$  is the position parameter (m).

By measuring the shift of the markers, the ‘‘Kirkendall displacement’’ can be determined over the entire diffusion zone and, subsequently, a displacement curve can be constructed (Fig. 2). Levasseur and Philibert [6] proposed a method to obtain the Kirkendall velocity and the intrinsic diffusion coefficients from the displacement curve. Later, this analysis was developed further due mainly to the work of Cornet and Calais [2, 7] and of van Loo *et al.* [8].

The Kirkendall velocity can be found as

$$v = \frac{1}{2t} \left( y - x_0 \cdot \frac{dy}{dx_0} \right) \quad (2)$$

with  $x_0$  being the original location of the markers and  $y$  the displacement of the markers relative to  $x_0$ . As can be seen from equation (2), the position of the Kirkendall plane within the interdiffusion zone, as marked by inert markers placed at the initial interface ( $x_0 = 0$ ), is given by  $v_K = y/2t$  ( $v_K$  is the velocity of the markers placed at the initial contact interface). The intrinsic diffusion coefficients can be calculated with the following equation [8]:

$$\frac{D_A}{D_B} = \frac{1 + QC_A}{1 - QC_B(V_B/V_A)} \quad \text{with} \quad (3)$$

$$Q = \frac{v}{\tilde{D} \cdot (dC_A/dx)}$$

where

$$\tilde{D} = D_A \cdot V_B \cdot C_B + D_B \cdot V_A \cdot C_A \quad (4)$$

$\tilde{D}$  is the interdiffusion coefficient, which can be found from the measured concentration profile in the diffusion couple.

The present analysis provides means to determine intrinsic diffusion coefficients in a binary metallic system over the whole concentration range from, in

principle, one single experiment. To make this procedure clear let us for the sake of illustration consider the behaviour of inert markers in hypothetical binary systems in which a specific concentration dependence of diffusion coefficients is assumed.

## 2.2. The Kirkendall velocity and displacement of inert markers during binary interdiffusion

It may be recalled that for a binary A–B solid solution system with constant interdiffusion coefficient and equal partial molar volumes, the concentration distribution of, for example, component A across the interaction zone after a certain time,  $t$ , can be described by Fick’s second law:

$$\frac{\partial N_A}{\partial t} = \frac{\partial}{\partial x} \left( \tilde{D} \frac{\partial N_A}{\partial x} \right) \quad (5)$$

where  $N_A$  is the molar fraction of A. Since we assumed  $\tilde{D} = \text{constant}$ , the solution is given by an error function:

$$N_A = \frac{1}{2} \text{erfc} \left( \frac{x}{2\sqrt{\tilde{D}t}} \right) \quad (6)$$

and the corresponding intrinsic diffusion coefficients  $D_A$  and  $D_B$  are concentration dependent as it automatically follows from equation (4).

The relation between the Kirkendall velocity and marker displacement is given by equation (2). The original position of the marker,  $x_0$ , is defined as  $x_0 = x - y(x)$  with  $x$  being the marker position after interaction and  $y(x)$  is its displacement. For the Kirkendall velocity  $v(x)$ , equation (2) can be written as

$$2tv(x) = g(x) = y(x) + [g(x) - x] \frac{dy}{dx}. \quad (7)$$

The last equation has a singularity for  $x = 2vt$ , which corresponds to the position of the Kirkendall plane. The solution for this first-order differential equation is given by

$$y(x) = \frac{1}{\mu(x)} \left( \mu(x_0)y(x_0) + \int_{x_0}^x \mu(\xi) \frac{g(\xi)}{g(\xi) - \xi} d\xi \right) \quad (8a)$$

with

$$\mu(x) = \exp \left[ \int \frac{1}{g(x) - x} dx \right] \quad (8b)$$

and can be found numerically using an appropriate computer program (e.g. Mathematica v3.0).

If now, for instance, the ratio of the intrinsic diffusivities of the components  $D_A/D_B$  is assumed to be constant, then the Kirkendall velocity at position  $x$  inside the diffusion zone can be found by combining equations (1) and (6):

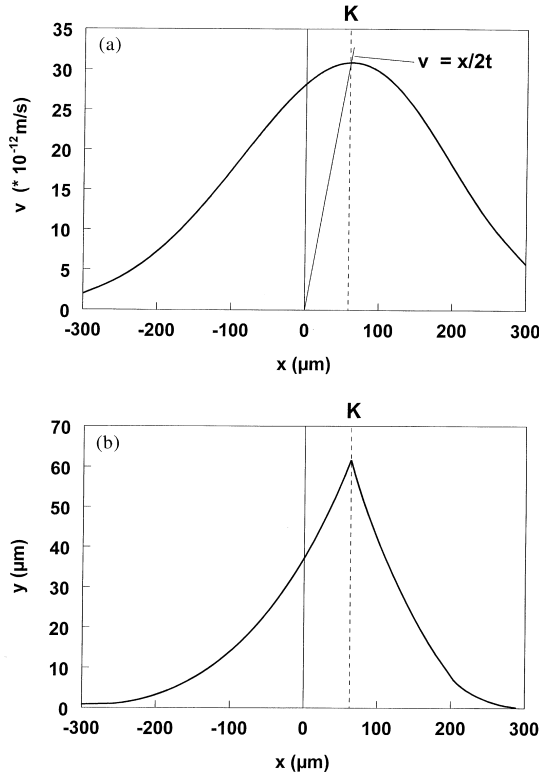


Fig. 3. (a) The Kirkendall velocity and (b) the Kirkendall displacement in a hypothetical A–B diffusion system ( $V_A = V_B$ ) with a constant interdiffusion coefficient  $\bar{D} = 10^{-14} \text{ m}^2/\text{s}$  and constant ratio of intrinsic diffusivities  $D_A/D_B = 3$  ( $t = 10^6 \text{ s}$ ); K indicates the Kirkendall plane.

$$v = \bar{D} \left( \frac{\frac{D_A}{D_B} - 1}{N_A + N_B \frac{D_A}{D_B}} \right) \left( \frac{-1}{\sqrt{\pi}} \frac{1}{2\sqrt{\bar{D}t}} \exp \left[ - \left( \frac{x}{2\sqrt{\bar{D}t}} \right)^2 \right] \right). \quad (9)$$

The position of the Kirkendall plane,  $x_K$ , is defined by  $v = x_K/2t$  and can be determined graphically as the intersection point of the velocity curve and the line  $v = x/2t$ .

Figure 3 shows the Kirkendall velocity and displacement curves obtained with the assumptions listed above, taking  $\bar{D} = 10^{-14} \text{ m}^2/\text{s}$ ,  $D_A/D_B = 3$  and  $t = 10^6 \text{ s}$ . As it was expected based on the consideration of Philibert [9], the maximum of the velocity curve and the displacement curve both coincide with the position of the Kirkendall plane. This type of marker behaviour was for a long time a generally accepted feature of the manifestation of the Kirkendall effect in binary solid solution systems. However, Cornet and Calais [2, 7] have demonstrated that this is not necessarily true. It can be illustrated by the following example.

Let us again suppose that the interdiffusion coefficient in a hypothetical binary solution system is

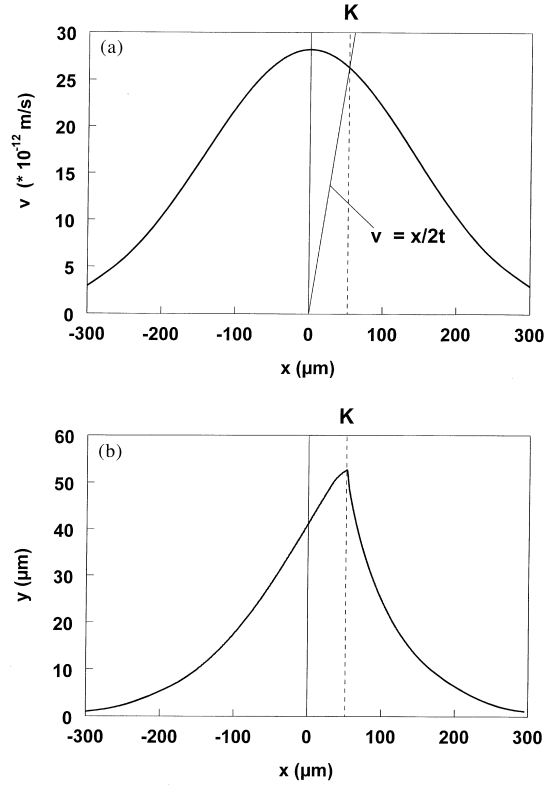


Fig. 4. (a) The Kirkendall velocity and (b) the Kirkendall displacement in a hypothetical A–B diffusion system ( $V_A = V_B$ ) with a constant interdiffusion coefficient  $\bar{D} = 10^{-14} \text{ m}^2/\text{s}$  and constant difference of intrinsic diffusivities  $D_A - D_B = 10^{-14} \text{ m}^2/\text{s}$  for the interaction time  $10^6 \text{ s}$ ; K indicates the Kirkendall plane.

constant and equal to  $10^{-14} \text{ m}^2/\text{s}$ . But now we assume that the difference between the intrinsic diffusivities of the components is constant, e.g.  $D_A - D_B = 10^{-14} \text{ m}^2/\text{s}$ . In this particular case, the Kirkendall velocity can be found in a similar way as in the previous example:

$$v = (D_A - D_B) \left( \frac{-1}{\sqrt{\pi}} \frac{1}{2\sqrt{\bar{D}t}} \exp \left[ - \left( \frac{x}{2\sqrt{\bar{D}t}} \right)^2 \right] \right) \quad (10)$$

and the displacement curve can be calculated using the procedure explained above. These constructions are given in Figs 4(a) and (b). One can see that the maximum of the Kirkendall velocity on the one hand and the maximum of the displacement and the position of the Kirkendall plane on the other hand do not coincide.

Before terminating this part of the demonstration, one further observation relevant to the problem challenged by the present study has to be mentioned. In Fig. 5 three velocity curves for hypothetical binary A–B solution systems are presented. The intrinsic diffusion coefficients are chosen arbitrarily in such a way that at the A-side of the

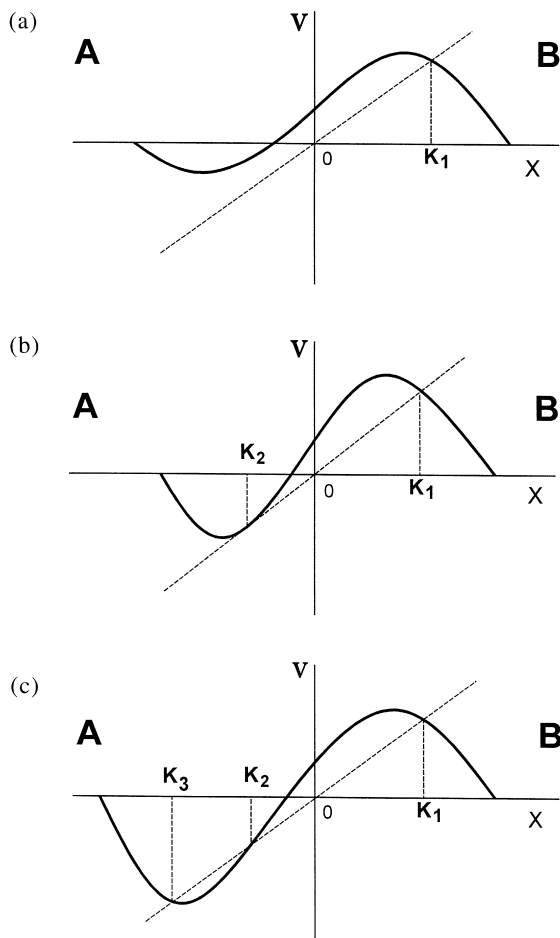


Fig. 5. The Kirkendall velocity in a hypothetical A–B diffusion system, in which the intrinsic diffusion coefficients of A and B are chosen arbitrarily in such a way that on one side of the diffusion zone A is the faster diffusing component and on the other side B has the highest diffusivity. One (a), two (b) or three (c) “Kirkendall” planes ( $K_1, K_2, K_3$ ) can emerge.

interdiffusion zone, A is the fastest diffusing component and on the other side, component B has the highest diffusivity. It can be seen that under such assumptions, the straight line  $v = x/2t$  may have one, two or three intersections with the velocity curve. In a translated sense, this would mean that in such a diffusion zone, one, two or three “Kirkendall planes”, originated from the initial interface marked, for example, by inert particles, could be expected. In this regard, it is interesting that Cornet and Calais [2] also showed hypothetical examples with multiple maxima on the velocity curve, in which the appearance of two or more “Kirkendall planes” is possible.

The conclusion drawn in the present theoretical analysis has led us to believe that “multiple Kirkendall planes” may emerge in a binary diffusion couple. The question is whether in “real” completely miscible binary systems this situation actually can occur.

Table 1. Diffusion couples analysed in the present work

| Diffusion couple   | Annealing temperature (°C) | Annealing time (h) |
|--------------------|----------------------------|--------------------|
| Ni/Pd              | 900                        | 770                |
| Ni/Pd              | 1000                       | 400                |
| Ni/Pd              | 1050                       | 196                |
| Ni/Pd              | 1100                       | 196                |
| Ni/Pd              | 1200                       | 40                 |
| Ni/Ni + 30 at.% Pd | 1100                       | 196                |
| Ni/Ni + 70 at.% Pd | 1100                       | 196                |
| Pd/Ni + 30 at.% Pd | 1100                       | 196                |
| Pd/Ni + 70 at.% Pd | 1100                       | 196                |
| Fe/Pd              | 1100                       | 143                |
| Multi-foil Ni/Pd   | 1100                       | 121                |
| Multi-foil Fe/Pd   | 1100                       | 144                |

3. EXPERIMENTAL PROCEDURE

Nickel (99.99%), palladium (99.99%) and iron (99.98%) supplied by Goodfellow (UK) were used as starting materials. A number of Ni–Pd alloys were melted in an arc furnace under argon atmosphere using a non-consumable tungsten electrode. The ingots were remelted three times to improve their homogeneity. Recrystallization and grain growth were accomplished by annealing in vacuum at 1050°C for 16–24 h. The grain size in the material after the treatment was in the range of 150–200 μm.

The diffusion couples were prepared and heat treated in a vacuum furnace ( $5 \times 10^{-7}$  mbar) under an external load of approximately 5 MPa for varying times and various temperatures. Small particles ( $\approx 0.3 \mu\text{m}$ ) of thorium dioxide ( $\text{ThO}_2$ ) were used as fiducial (Kirkendall) markers. Table 1 gives an overview of the diffusion couples made in the present investigation.

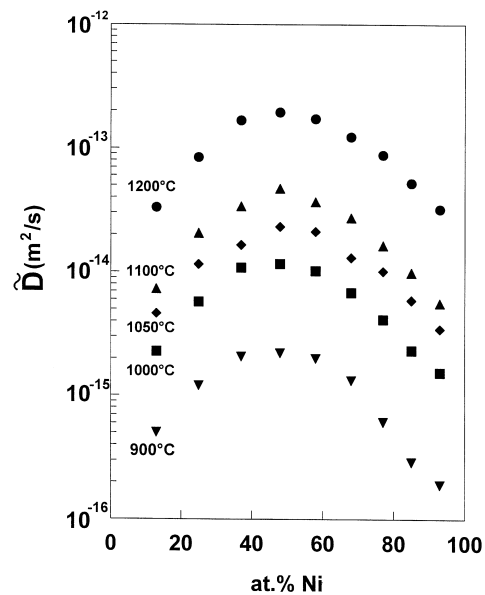


Fig. 6. Concentration dependence of the interdiffusion coefficient  $\tilde{D}$  in the Ni–Pd system at different temperatures.

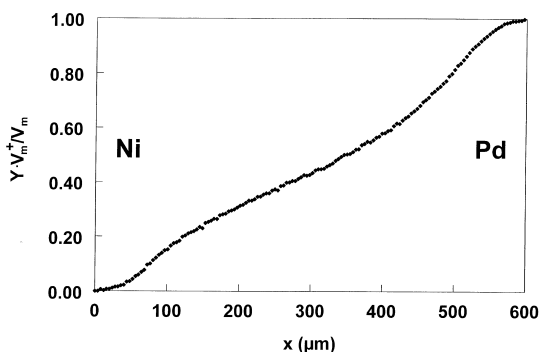


Fig. 7. Penetration curve of a Ni/Pd diffusion couple (1100°C; 196 h) constructed according to the Sauer and Freise method.  $Y = (N_{Pd} - N_{Pd}^-) / (N_{Pd}^+ - N_{Pd}^-)$ ;  $V_m^+$  is the molar volume of Pd.

After annealing and standard metallographic preparation, the diffusion couples were examined by optical microscopy, scanning electron microscopy (SEM) and electron probe microanalysis (EPMA). Concentration profiles across the interaction zones were measured and the behaviour of the inert ThO<sub>2</sub> markers during interdiffusion was studied.

#### 4. EXPERIMENTAL RESULTS AND DISCUSSION

##### 4.1. Diffusion in the nickel–palladium system

The concentration dependence of the interdiffusion coefficient at various temperatures was

obtained by analysing the annealed Ni/Pd couples (Fig. 6). Concentration profiles measured with EPMA across the diffusion zones were evaluated using the Sauer and Freise method [10]. This method takes into account the total volume change during interdiffusion. As a representative example, the penetration curve of a Ni–Pd diffusion couple annealed for 196 h at 1100°C constructed according to the Sauer and Freise method is shown in Fig. 7. Molar volumes of the Ni–Pd solid solution were calculated with the lattice parameter values of Ref. [11].

The present results are similar to the observation reported by Borovskiy *et al.* [12]. The maximum of the concentration dependence coincides (within experimental accuracy) with the minimum on the liquidus of the binary Ni–Pd system (at 45–50 at.% of Ni). This supports the idea that in the proximity of the melting point the amount of thermal vacancies increases, resulting in the enhancement of the atomic mobilities.

The experimentally determined interdiffusion coefficients for several alloy compositions were plotted as a function of the reciprocal temperature (Arrhenius coordinates) and the apparent activation energies and pre-exponential factors for interdiffusion in the Ni–Pd solid solutions were calculated. The results are summarized in Table 2.

In addition, the concentration dependence of the interdiffusion at 1100°C was derived from the experiments on incremental diffusion couples (Table 1). The results are presented in Fig. 8. One can see

Table 2. Activation energy,  $Q$ , and the pre-exponential factor,  $D_0$ , for interdiffusion in the Ni–Pd system at 900–1200°C and intrinsic diffusion coefficients of the components in the Ni–Pd solid solution determined in the present study at 1100°C

| Interdiffusion at 900–1200°C    |                                          |                                          |                                      |                                          |                                          |
|---------------------------------|------------------------------------------|------------------------------------------|--------------------------------------|------------------------------------------|------------------------------------------|
| at.% Ni                         | $Q$ (kJ/mol)                             |                                          | $D_0$ ( $10^{-5}$ m <sup>2</sup> /s) |                                          |                                          |
| 15.4                            | 233.8                                    |                                          | 8.6                                  |                                          |                                          |
| 23.1                            | 234.2                                    |                                          | 15.5                                 |                                          |                                          |
| 32.2                            | 217.4                                    |                                          | 5.5                                  |                                          |                                          |
| 42.2                            | 209.3                                    |                                          | 3.8                                  |                                          |                                          |
| 52.1                            | 209.9                                    |                                          | 4.2                                  |                                          |                                          |
| 62.1                            | 202.7                                    |                                          | 1.8                                  |                                          |                                          |
| 73.5                            | 204.0                                    |                                          | 1.2                                  |                                          |                                          |
| 86.6                            | 212.1                                    |                                          | 1.1                                  |                                          |                                          |
| Intrinsic diffusion at 1100°C   |                                          |                                          |                                      |                                          |                                          |
| Incremental couples             |                                          |                                          | Multi-foil couple                    |                                          |                                          |
| at.% Ni at K-plane <sup>a</sup> | $D_{Ni}$ ( $10^{-14}$ m <sup>2</sup> /s) | $D_{Pd}$ ( $10^{-14}$ m <sup>2</sup> /s) | at.% Ni                              | $D_{Ni}$ ( $10^{-14}$ m <sup>2</sup> /s) | $D_{Pd}$ ( $10^{-14}$ m <sup>2</sup> /s) |
| 17.6                            | 1.8                                      | 2.0                                      | 6.6                                  | 0.33                                     | 0.33                                     |
| 40.3                            | 4.9                                      | 6.5                                      | 13                                   | 0.69                                     | 0.97                                     |
| 51.6                            | 3.4                                      | 4.7                                      | 25                                   | 1.98                                     | 2.34                                     |
| 58.5                            | 3.3                                      | 4.3                                      | 37                                   | 3.53                                     | 3.85                                     |
| 82.6                            | 0.38                                     | 0.81                                     | 48                                   | 3.74                                     | 4.97                                     |
|                                 |                                          |                                          | 58                                   | 2.97                                     | 4.51                                     |
|                                 |                                          |                                          | 68                                   | 1.98                                     | 3.11                                     |
|                                 |                                          |                                          | 77                                   | 0.72                                     | 2.08                                     |
|                                 |                                          |                                          | 85                                   | 0.22                                     | 1.19                                     |
|                                 |                                          |                                          | 92                                   | 0.15                                     | 0.64                                     |

<sup>a</sup> Concentration at the position of the Kirkendall plane.

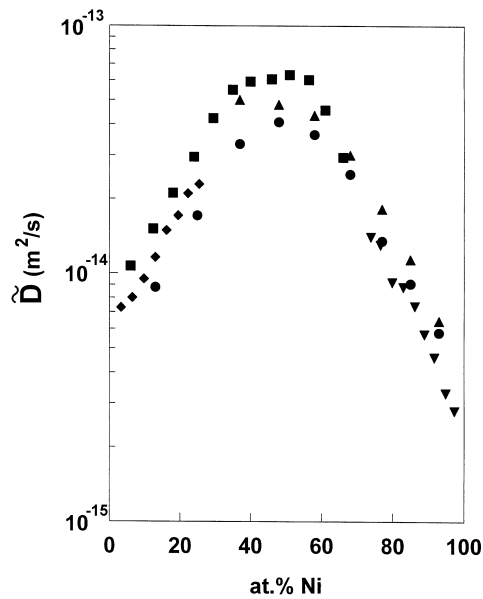


Fig. 8. Interdiffusion coefficients in the Ni–Pd system at 1100°C obtained with different diffusion couples: ●, Ni/Pd; ▲, Ni/(Ni + 70 at.% Pd); ▼, Ni/(Ni + 30 at.% Pd); ◆, Pd/(Ni + 70 at.% Pd); ■, Pd/(Ni + 30 at.% Pd).

that these values are consistent with those obtained by investigating the diffusion couples with pure Ni and Pd as end members. In other words, the inter-

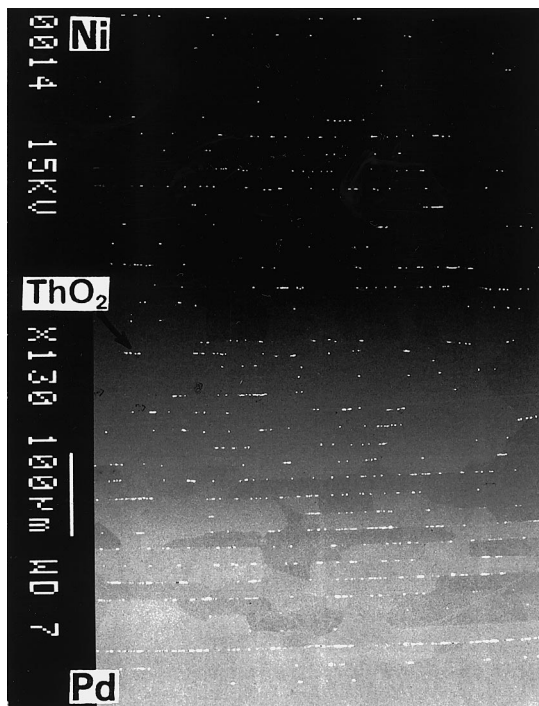


Fig. 9. Backscattered electron image of a Ni/Pd multi-foil diffusion couple annealed at 1100°C for 121 h in vacuum. The rows of ThO<sub>2</sub> particles used as fiducial markers correspond to the interfaces between the initial foils. Note: no pore formation after the heat treatment.

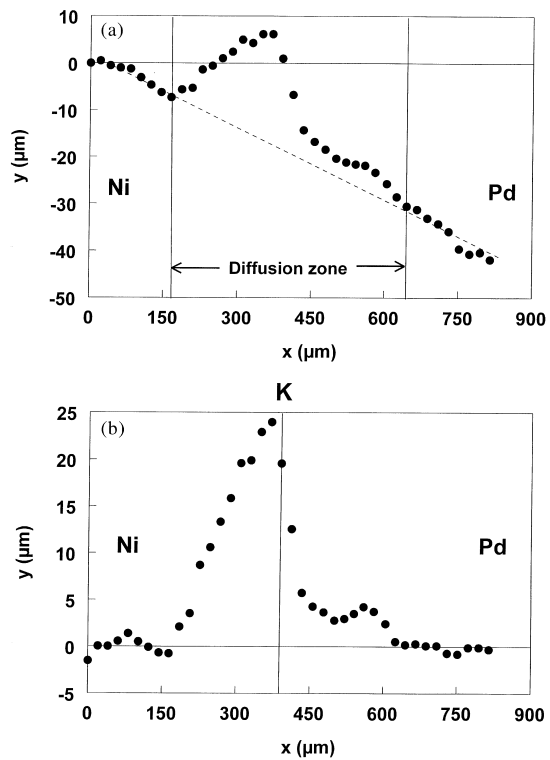


Fig. 10. Displacement curves [ $y(x)$ ] (a) determined experimentally and (b) corrected for plastic deformation for a Ni/Pd multi-foil diffusion couple annealed at 1100°C for 121 h (K indicates the Kirkendall plane).

diffusion coefficient is a single-valued function of composition. This implies that under the experimental conditions used, local thermodynamic equilibrium for the formation of defects (namely vacancies) within the diffusion zone is virtually established.

From the measured penetration curves in these couples the intrinsic diffusion coefficients  $D_{\text{Ni}}$  and  $D_{\text{Pd}}$  were determined for the concentrations of the Ni–Pd solid solution corresponding to the position of the Kirkendall plane (Table 2).

More information on intrinsic diffusivities in this system at 1100°C was obtained from the “multi-foil” experiment. Twenty foils (20 µm thick) of Pd and 19 foils (21 µm thick) of Ni were pressed together between the plan-parallel slices ( $\approx 1.0$  mm thick) of pure metals (end members). ThO<sub>2</sub> particles ( $\approx 0.3$  µm) were used as fiducial markers between the foils. The couple was annealed at 1100°C first for 9 h, cross-sectioned and analysed in order to determine the distances between the original foil interfaces. Then, the sample was annealed further at this temperature for up to 121 h. Figure 9 shows a cross-section of the couple after the heat treatment. No pore formation was observed in the diffusion zone. The ThO<sub>2</sub> markers are clearly visible as straight rows of inclusions exhibiting a “white” contrast in the backscattered electron micrograph. From the concentration profile measured across the

interaction zone, the interdiffusion coefficients for various compositions of the Ni–Pd solid solution at 1100°C were computed using the Sauer–Freise method. As it was expected, the results are compatible with the values found by analysing the incremental couples and the couples with the pure metals as end members.

The displacement of markers within the diffusion zone was calculated taking the first “marked” plane at the pure Ni-side of the couple as a reference (Fig. 10). The original marker positions were determined using the average values of the foil thick-

nesses (nickel or palladium) in the parts of the couple where no interdiffusion has taken place yet after annealing at this temperature for 9 h. It turned out that the markers located outside the interdiffusion zone are also shifted. Obviously, this is a direct outcome of the sample deformation (creep) caused by the pressure applied during the joining and annealing. To take into account the possible effect of plastic deformation and determine the genuine Kirkendall displacement, a correction procedure similar to that proposed by Heumann and Grundhoff [13] was used. The approach is quite simple. As a first approximation, the deformation rate of the end members of the couple is assumed to be equal and constant. In such a case the line in Fig. 10(a) connecting the marker position inside the “unreacted” parts of the couple, i.e. outside the interdiffusion zone, represents the displacement of the markers resulting from the plastic deformation. The difference between the apparent marker displacement and the value corresponding to this “baseline” gives the actual Kirkendall shift. In this manner the displacement curve shown in Fig. 10(b) was constructed. It can be seen that the displacement of markers has a positive value, indicating that Pd is the fastest diffusing component over the composition range studied. The maximum of the displacement, which is situated in the vicinity of the Kirkendall plane, was found to be  $24 \pm 2 \mu\text{m}$ .

Further, the intrinsic diffusion coefficients were calculated for various concentrations of the binary Ni–Pd alloys using the procedure discussed in the preceding section [equations (2)–(4)]. These values are listed in Table 2 and presented graphically in Fig. 11. The results are, in general, consistent with those obtained in the experiments on the incremental diffusion couples. It is relevant to notice that the intrinsic diffusion coefficient of Ni and Pd in the binary solid solution as a function of concentration goes through a maximum. That is somewhat similar to the behaviour found for the interdiffusion in this system. The maximum of the intrinsic diffusivities is also situated near the equatomic composition, which corresponds to the minimum of the melting point in this system.

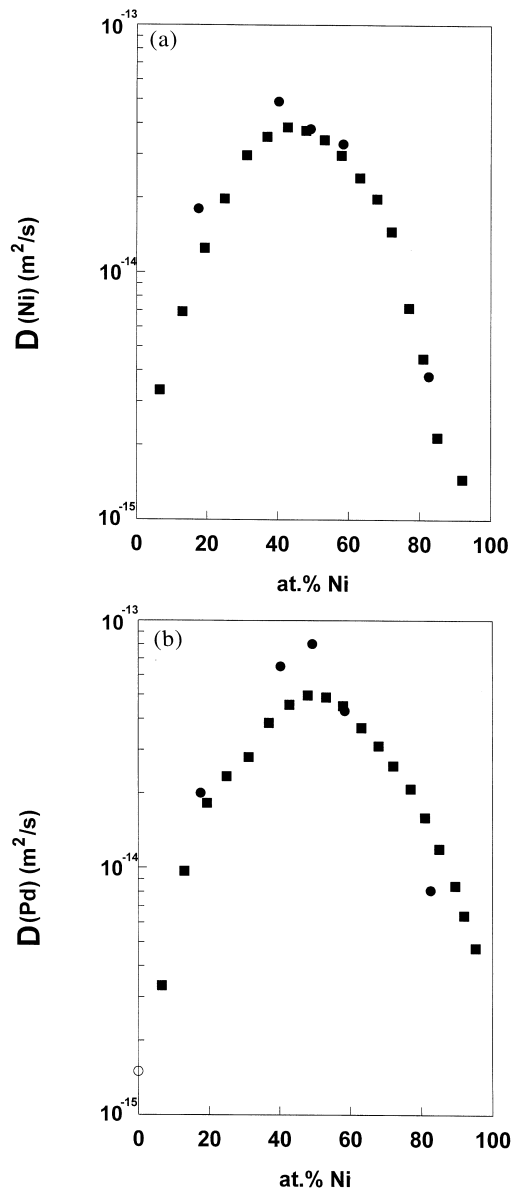


Fig. 11. Intrinsic diffusion coefficients (a) of nickel,  $D_{\text{Ni}}$ , and (b) of palladium,  $D_{\text{Pd}}$ , in the Ni–Pd alloys at 1100°C obtained with incremental couples (●) and derived from the multi-foil experiment (■). The value for the self-diffusion coefficient of palladium [14] is given for comparison (○).

#### 4.2. Diffusion in the Fe–Pd solid solution at 1100°C

Contrary to the Ni–Pd system, no data on the variation of lattice spacing in iron–palladium alloys are available. We assumed that the molar volume of the f.c.c. solid solution as a function of the atomic fraction of Pd in this system follows Vegard’s law. The interdiffusion data in the Fe–Pd solid solution at 1100°C were obtained by analysing the concentration profile in the annealed Fe/Pd couple using the conventional Matano–Boltzmann analysis. The experimentally determined interdiffusion coefficients are given in Table 3 and Fig. 12.

Table 3. Interdiffusion coefficient,  $\tilde{D}$ , in the Fe–Pd alloys determined experimentally at 1100°C and calculated using Darken's analysis [equation (4)]. The tracer diffusivities and thermodynamic data for the Fe–Pd solid solution are taken from Refs [14, 17–19]

| at.% Fe | $\tilde{D}$ ( $10^{-14}$ m <sup>2</sup> /s) experimental | Thermodynamic factor, $\Phi$ | Intrinsic diffusivity                    |                                          | $\tilde{D}$ ( $10^{-14}$ m <sup>2</sup> /s) calculated |
|---------|----------------------------------------------------------|------------------------------|------------------------------------------|------------------------------------------|--------------------------------------------------------|
|         |                                                          |                              | $D$ (Fe) ( $10^{-14}$ m <sup>2</sup> /s) | $D$ (Pd) ( $10^{-14}$ m <sup>2</sup> /s) |                                                        |
| 0       | –                                                        | 1                            | 0.27                                     | 0.15                                     | 0.27                                                   |
| 9.5     | 1.16                                                     | 1.3                          | 0.43                                     | 0.38                                     | 0.42                                                   |
| 21.8    | 3.43                                                     | 4.8                          | 2.95                                     | 2.48                                     | 2.82                                                   |
| 31.7    | 6.13                                                     | 4.7                          | 4.61                                     | 3.10                                     | 4.13                                                   |
| 45.0    | 3.71                                                     | 3.5                          | 4.28                                     | 2.80                                     | 3.61                                                   |
| 51.6    | 2.61                                                     | 3.2                          | 3.59                                     | 2.20                                     | 2.87                                                   |
| 61.0    | 1.40                                                     | 1.2                          | 1.16                                     | 0.68                                     | 0.87                                                   |
| 71.8    | 0.57                                                     | 0.57                         | 0.41                                     | 0.27                                     | 0.31                                                   |
| 80.9    | 0.33                                                     | 0.45                         | 0.21                                     | 0.16                                     | 0.17                                                   |
| 89.9    | 0.28                                                     | 0.38                         | 0.094                                    | 0.078                                    | 0.081                                                  |
| 100     | –                                                        | 1                            | 0.10                                     | 0.10                                     | 0.10                                                   |

These are in accordance with results reported by Gomez *et al.* [15].

At this point it is appropriate to remember that the intrinsic diffusion coefficient,  $D_i$ , is related to the tracer diffusion coefficient,  $D_i^*$ , in the homogeneous phase of the same composition. For the binary A–B system the relationship is given by†

$$D_A = D_A^* \cdot \frac{V_m}{V_B} \left[ \frac{d \ln a_A}{d \ln N_A} \right] \quad (11)$$

with  $(d \ln a_A)/(d \ln N_A) = (d \ln a_B)/(d \ln N_B)$  being the thermodynamic factor ( $a_A$  and  $a_B$  are the chemical activity of components A and B, respectively).  $V_m$  and  $V_B$  are the molar and partial molar volumes, respectively.

Thermodynamic activities of iron in Fe–Pd alloys were determined from oxidation experiments at 1200–1400°C by Aukrust and Muan [17]. Later, Alcock and Kubik [18] performed a comprehensive study of the thermodynamic properties of Fe–Pd solid solutions over the temperature range 700–1000°C using the e.m.f. method. It is interesting to mention some peculiarities in the thermodynamic behaviour of the Fe–Pd system in this temperature range. Iron-rich solid solutions exhibit positive deviations from Raoultian behaviour for the activity of iron and negative deviation for the activity of the palladium. Palladium-rich solid solutions, on the other hand, exhibit negative deviations from Raoult's law for the activity of both elements.

By extrapolating the reported e.m.f. values to 1100°C and correcting for the non-stoichiometry of wüstite [19] used as an electrode material, the activities of iron in the Fe–Pd alloys were derived. The

thermodynamic factor at this temperature was calculated for various compositions (Table 3).

Tracer diffusion coefficients in the Fe–Pd system at 1100–1250°C were measured by Fillion and Calais [14]. Using the data at 1100°C and values of the thermodynamic factor, the corresponding intrinsic and, then, interdiffusion coefficients were computed with equations (4) and (11) (Table 3). One sees that the experimentally determined and calculated values of the interdiffusion coefficients are in agreement (Fig. 12).

The intrinsic diffusivities of the components in the Fe–Pd solid solution at 1100°C were also obtained from the “multi-foil” couple experiment. To this end, 24 foils of Pd (20  $\mu$ m) and eight foils of Fe (25  $\mu$ m) were pressed together between the

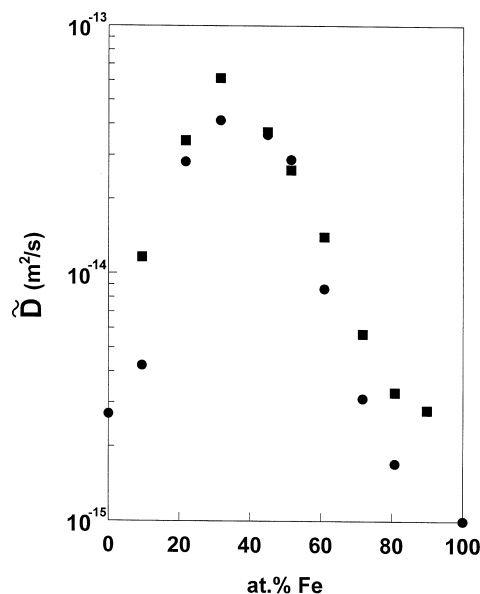


Fig. 12. Concentration dependence of the interdiffusion coefficient  $\tilde{D}$  in the Fe–Pd system at 1100°C: ■, determined experimentally in the present work using the Matano–Boltzmann analysis; ●, computed with equation (4) using thermodynamic and diffusion data of Refs [14, 17–19].

† Often a so-called “vacancy wind term” (or Manning’s correction) is added to equation (11) [16]. However, we found that under the experimental conditions used in the present work, the possible correction in the case of the Fe–Pd would be within the limits of experimental accuracy. Therefore, this correction factor will not be introduced here.

slices of pure end members and annealed in vacuum. Again,  $\text{ThO}_2$  particles were used as inert markers. Using the procedure described above, the displacement curve was constructed and intrinsic diffusion coefficients of Fe and Pd were determined. The results are presented in Fig. 13 along with the values calculated from the tracer diffusivities of the species and thermodynamic data.

The maximum in the interdiffusion rate in the Fe–Pd system was found at approximately 30–35 at.% of iron. This is quite far from the position of the minimum on the liquidus curve on the Fe–Pd phase diagram [3] (which is at about 50 at.% of

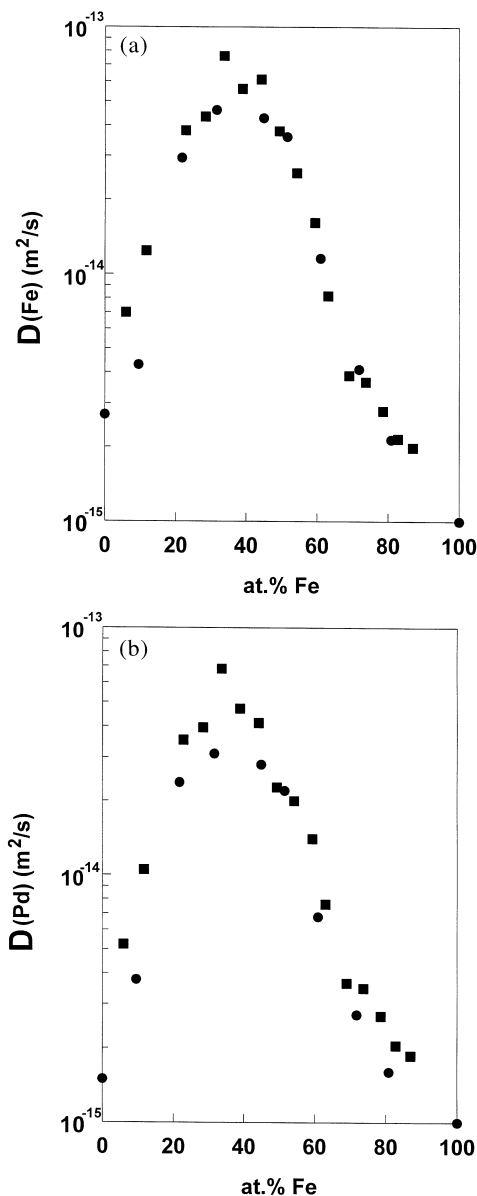


Fig. 13. Intrinsic diffusion coefficient (a) of iron,  $D_{\text{Fe}}$ , and (b) of palladium,  $D_{\text{Pd}}$ , in the Fe–Pd solid solution at 1100°C: ■, determined experimentally using the multi-foil technique; ●, calculated using data of Refs [14, 17–19].

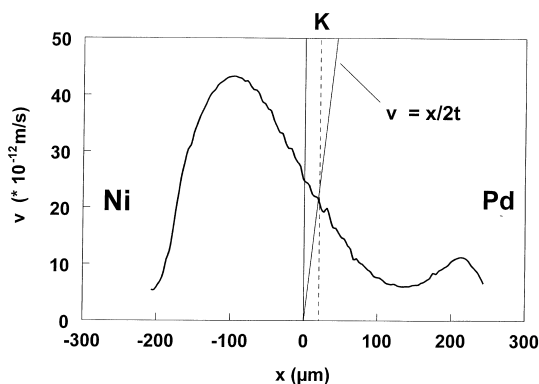


Fig. 14. Marker velocity curve in the Ni/Pd multi-foil diffusion couple annealed at 1100°C for 121 h calculated using experimental data of the present study. Note: the Matano plane is located at  $x = 0$ .

Fe). The maximum of the concentration dependence of intrinsic diffusivities in the Fe–Pd alloys is also located near the Fe content of about 30–35%. However, the tracer diffusion coefficient as a function of concentration of the solid solution was reported to go through a maximum, which is close to the equatomic composition [14]. It is not readily apparent why the Ni–Pd and Fe–Pd systems behave differently with regard to the concentration dependence of the interdiffusion rate. We believe that in the case of the Fe–Pd solid solution the appearance of the maximum on the  $\tilde{D}$  vs composition curve at 1100°C cannot be explained solely in terms of the proximity of the melting point. It can be conjectured that a tendency towards ordering, which in this system is manifested by the formation of the intermetallic phases,  $\text{FePd}$  and  $\text{FePd}_3$ , at lower temperature [3], contributes (in terms of the thermodynamic factor) to the overall interdiffusion process. This can be appreciated from the data in Table 3.

#### 4.3. Kirkendall effect in the Ni–Pd, Fe–Pd and Ti–Ni couples

In Section 2 we have seen that the number of “Kirkendall planes” that emerge in the interaction zone of a binary diffusion couple can be found from the marker (Kirkendall) velocity curve. Figure 14 shows the experimentally determined velocity curve in the case of the annealed Ni/Pd multi-foil couple. One can see that the straight line  $v = x/2t$ , which is the velocity of the markers originating from the initial interface [ $x_0 = 0$  in equation (2)], intersects this curve once. The same result was found for the Fe/Pd multi-foil diffusion couple. Therefore, only one Kirkendall plane should be found inside the interaction zone in these systems.

However, as mentioned in Section 1 the appearance of two “Kirkendall planes” marked by  $\text{ThO}_2$  particles was observed inside the Ti/Ni multiphase

Table 4. Integrated diffusion coefficient,  $D_{\text{int}}$ , and the ratio of the intrinsic diffusivities ( $K = D_{\text{Ni}}/D_{\text{Ti}}$ ) in the binary Ti–Ni intermetallics at 850°C together with the layer thicknesses ( $\Delta x$ ) and the calculated marker velocity,  $v$ , values in the phase layers formed in the Ti/Ni couple after interaction (196 h; 850°C). The original experimental data were taken from Ref. [21]

| Compound           | $D_{\text{int}}$ ( $10^{-16}$ m <sup>2</sup> /s) | $K = D_{\text{Ni}}/D_{\text{Ti}}$ | $\Delta x$ ( $\mu\text{m}$ ) | $v$ ( $10^{-12}$ m <sup>2</sup> /s) |
|--------------------|--------------------------------------------------|-----------------------------------|------------------------------|-------------------------------------|
| TiNi <sub>3</sub>  | 1.7                                              | > 20                              | 8                            | 85                                  |
| TiNi               | 22                                               | ~ 15                              | 56                           | 68                                  |
| Ti <sub>2</sub> Ni | 0.67                                             | ~ 10                              | 10                           | 9                                   |

reaction zone (Fig. 1). This phenomenon can also be explained in terms of a marker velocity curve. In the case of a multiphase binary system A–B, the marker velocity can be expressed as (see Appendix):

$$v = \frac{K - 1}{KN_B + N_A} \frac{D_{\text{int}}}{\Delta x} \quad (12)$$

where  $K = D_A/D_B$  is the ratio of the intrinsic diffusivities of the A and B,  $D_{\text{int}}$  is the integrated diffusion coefficient [20] (m<sup>2</sup>/s),  $N_A$  and  $N_B$  are the molar fraction of A and B, respectively, and  $\Delta x$  is the thickness of the intermetallic compound (m). Using data of Ref. [21], the integrated diffusion coefficients and the ratio of the intrinsic diffusivities for the Ti–Ni intermetallics (TiNi<sub>3</sub>, TiNi and Ti<sub>2</sub>Ni) at 850°C were calculated (Table 4) and the marker velocity curve for the Ti/Ni diffusion couple was constructed (Fig. 15). One can see that the line  $v = x/2t$  intersects this curve twice. This implies that two “Kirkendall planes” should be expected. Indeed, two planes marked by ThO<sub>2</sub> particles were experimentally observed in this diffusion couple.

## 5. CONCLUDING REMARKS

The “multi-foil” diffusion couple technique proved to be a valuable experimental method for studying intrinsic diffusion and the Kirkendall effect in binary solid solutions. It allows us to deduce the concentration dependence of the intrinsic diffusion coefficient from, in principle, one single experiment.

From a fundamental point of view, the diffusion

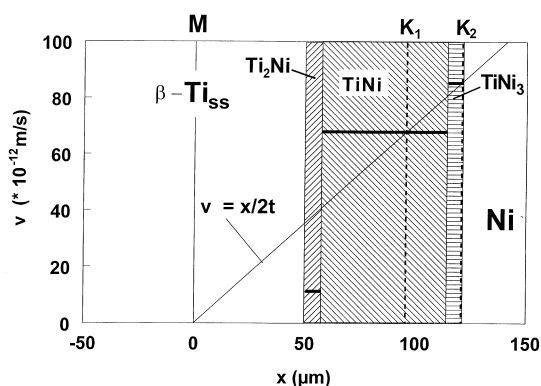


Fig. 15. Marker velocity curve in the multiphase Ti/Ni diffusion couple after annealing at 850°C for 196 h calculated using experimental data of Ref. [21]. Note: the Matano plane is located at  $x = 0$  ( $\beta$ -Ti<sub>ss</sub> = b.c.c. solid solution).

processes in solid solutions of binary systems exhibiting a minimum on the liquidus curve, show special features with regard to the concentration dependence of the diffusion coefficients. An examination of the Ni–Pd and Fe–Pd systems performed in the present work confirmed a strong dependence of the inter-, intrinsic and self-diffusion coefficients on the alloy composition. This is reflected by the presence of a distinct maximum on a concentration dependence curve. It appears that, in general, the position of the maximum cannot be explained only in terms of proximity of the melting point and availability of thermal vacancies, but also effects of thermodynamic nature are of importance, like a tendency towards ordering.

The number of “Kirkendall planes” inside the interaction zone of a binary diffusion couple can be deduced from the marker velocity curve. Multiple Kirkendall planes in the multiphase Ti–Ni system have been predicted and found at 850°C. However, it is important to realize that the problem, challenged by this study, remains. Although it was demonstrated (theoretically) that multiple “Kirkendall planes” might emerge within a single-phase (solid solution) interdiffusion zone, the vital experiment that confirms this statement has still to be found. In this respect, diffusion studies on ternary metallic systems provide the necessary framework to find clear-cut evidence of the “separation” of the Kirkendall planes (as marked by inert markers) during interdiffusion in single-phase systems, because one extra degree of freedom is available to control the direction of the vacancy fluxes. Currently, this type of research is conducted in our laboratory.

*Acknowledgements*—We are indebted to the following people from the Eindhoven University of Technology, whose advice and encouragement helped us to resolve some of the more serious problems we encountered: dr.ir. J. K. M. Jansen, dr.ir. P. G. Th. van der Varst and dr. S. Yu. Shulepov. We were most fortunate to have at our disposal the skill of H. A. M. van der Palen, who assisted with the experimental work. A special thanks goes to Professor Ü. E. Ugaste (University of Tallinn, Estonia) for his valuable contribution especially at the early stage of the study.

## REFERENCES

- van Loo, F. J. J., Pieraggi, B. and Rapp, R. A., *Acta metall. mater.*, 1990, **38**, 530.

2. Cornet, J.-F. and Calais, D., *J. Phys. Chem. Solids*, 1972, **33**, 1675.
3. Massalski, T. B., Murray, J. I., Bennet, L. H. and Baker, H. (ed.), *Binary Alloy Phase Diagram*. ASM, Metals Park, OH, 1986.
4. Heumann, Th. and Walther, G., *Z. Metallk.*, 1957, **48**, 151.
5. Darken, L. S., *Trans. Am. Inst. Min. Engrs*, 1948, **175**, 184.
6. Levasseur, J. and Philibert, J., *Physica status solidi*, 1967, **21**, K1.
7. Cornet, J.-F., *J. Phys. Chem. Solids*, 1974, **35**, 1247.
8. van Loo, F. J. J., Bastin, G. F. and Rieck, G. D., *Sci. Sintering*, 1979, **11**, 9.
9. Philibert, J., *Atom Movements and Mass Transport in Solids*. Les Éditions de Physique, Les Ulis, 1991.
10. Sauer, F. and Freise, V., *Z. Elektrochem.*, 1962, **66**, 353.
11. Nash, A. and Nash, P., *Bull. Alloy Phase Diagrams*, 1984, **5**, 446.
12. Borovskiy, I. B., Marchukova, I. D. and Ugaste, Ü. E., *Fizika Metall. Metalloved.*, 1966, **22**, 43.
13. Heumann, Th. and Grundhoff, K. J., *Z. Metallk.*, 1972, **63**, 173.
14. Fillion, J. and Calais, D., *J. Phys. Chem. Solids*, 1977, **38**, 81.
15. Gomez, J.-P., Remy, C. and Calais, D., *Mém. scient. Revue Métall.*, 1973, **70**, 597.
16. Manning, J. R., *Acta metall.*, 1967, **15**, 817.
17. Aukrust, E. and Muan, A., *Acta metall.*, 1962, **10**, 555.
18. Alcock, C. B. and Kubik, A., *Acta metall.*, 1969, **17**, 437.
19. Darken, L. S. and Gurry, R. W., *J. Am. Chem. Soc.*, 1945, **67**, 1398.
20. Wagner, C., *Acta metall.*, 1969, **17**, 99.
21. Bastin, G. F., Ph.D. thesis, University of Technology, Eindhoven, The Netherlands, 1972.

#### APPENDIX

The material constant, integrated diffusion coefficient  $D_{\text{int}}$ , is defined for a diffusion-grown phase with a narrow homogeneity range (line compound) as the interdiffusion coefficient in this phase inte-

grated over its (unknown) homogeneity limits  $N'$  and  $N''$  ( $N$  is the molar fraction) [20]:

$$D_{\text{int}} = \int_{N'}^{N''} \tilde{D} \, dN. \quad (\text{A1})$$

The integrated diffusion coefficient can be easily obtained from the concentration profile [20]. If we assume that the (unknown) interdiffusion coefficient in the phase is constant, equation (A1) can be simplified to

$$D_{\text{int}} = \tilde{D}(N'' - N') = \tilde{D}\Delta N. \quad (\text{A2})$$

The marker velocity given by equation (1) can be written as

$$\begin{aligned} v &= V_A(D_A - D_B) \frac{\partial C_A}{\partial x} \\ &= \frac{V_A \cdot V_B}{V_m^2} (D_A - D_B) \frac{\partial N_A}{\partial x} \approx (D_A - D_B) \frac{\Delta N}{\Delta x} \end{aligned} \quad (\text{A3})$$

where  $V_A$  and  $V_B$  are the partial molar volumes of A and B, respectively,  $V_m$  is the molar volume of the compound and  $\Delta x$  is the thickness of the phase layer formed in a diffusion couple. Combining equations (A2) and (A3) and introducing the ratio of the intrinsic diffusivities  $K = D_A/D_B$ , the marker velocity can be expressed as

$$v = \frac{K - 1}{KN_B + N_A} \frac{D_{\text{int}}}{\Delta x}. \quad (\text{A4})$$

Since the homogeneity range of the line compound is supposed to be small, the integrated diffusion coefficient  $D_{\text{int}}$  and the ratio of the intrinsic diffusivities can be considered constant. Consequently, the velocity of markers within the line compound has a constant value.